3.11 Physiological Based Simulator Fidelity Design Guidance

PHYSIOLOGICAL BASED SIMULATOR FIDELITY DESIGN GUIDANCE

Tom "MACH" Schnell, Operator Performance Laboratory (OPL)
thomas-schnell@uiowa.edu

Nancy Hamel, Col. USAF (Ret), Advanced Infoneering, Inc.
nahamel@advancedinfoneering.com

Alex Postnikov, and Jaclyn Hoke, Rockwell Collins, Inc.
apostnik@rockwellcollins.com, jahoke@rockwellcollins.com

Angus "MAC" L. M. Thom McLean, III., ApotheoSys, Inc.
thom@apotheosys.com

Abstract. The evolution of the role of flight simulation has reinforced assumptions in aviation that the degree of realism in a simulation system directly correlates to the training benefit, i.e., more fidelity is always better. The construct of fidelity has several dimensions, including physical fidelity, functional fidelity, and cognitive fidelity. Interaction of different fidelity dimensions has an impact on trainee immersion, presence, and transfer of training. This paper discusses research results of a recent study that investigated if physiological-based methods could be used to determine the required level of simulator fidelity. Pilots performed a relatively complex flight task consisting of mission task elements of various levels of difficulty in a fixed base flight simulator and a real fighter jet trainer aircraft. Flight runs were performed using one forward visual channel of 40° field of view for the lowest level of fidelity, 120° field of view for the middle level of fidelity, and unrestricted field of view and full dynamic acceleration in the real airplane. Neuro-cognitive and physiological measures were collected under these conditions using the Cognitive Avionics Tool Set (CATS) and nonlinear closed form models for workload prediction were generated based on these data for the various mission task elements. One finding of the work described herein is that simple heart rate is a relatively good predictor of cognitive workload, even for short tasks with dynamic changes in cognitive loading. Additionally, we found that models that used a wide range of physiological and neuro-cognitive measures can further boost the accuracy of the workload prediction.

INTRODUCTION

The earliest development of simulators were directed towards familiarizing a student pilot with the basics of flight before the "real" instruction began in the aircraft. As the sophistication of aircraft and flight simulators increased, the utility of cockpit procedure trainers (CPTs) became clear – aircrew could learn the layout and function of the cockpit systems with greater efficiency on the ground than in the air. The incorporation of motion and visual systems allowed students to be introduced to even more sophisticated tasks and maneuvers prior to attempting them in the air. For certain tasks, such as delivering special ordinance or dealing with catastrophic systems failures, simulators provided the only way to prepare a pilot. This reliance on increasingly sophisticated simulators led to a belief that, in general, simulators should replicate as many aspects of the real-world as possible. For commercial aviation, this approach has produced simulators that can be certified to provide complete initial and recurrent aircrew qualification. Today, commercial aircraft flight simulators are considered a cornerstone of flight instruction and pilot certification. The development of modern simulators has evolved to embrace the most sophisticated dimensions of flight training and mission rehearsal.

In flight simulators, physical fidelity relates to the accuracy of the physical layout of the crew station and how closely the visual, auditory, haptic, vestibular, and flight dynamic stimuli mimic those that will be experienced in the real aircraft. Functional fidelity primarily relates to how accurately the simulated crew station equipment acts like the operational equipment and cognitive fidelity is a quantification of how closely the human factors effects of the virtual environment track with those that will be found when operating in the real aircraft.

Statement of Problem

Designers of virtual environments for mission readiness training are ill-equipped to deal with difficult cost-benefit trade-offs that may affect fidelity and training effectiveness or transfer of training. Interaction of different fidelity dimensions

has an impact on trainee immersion, presence, and buy-in [1,2]. Flight simulators need to be designed to achieve a specific training objective. If too much simulator fidelity is specified for the objective, the simulator will be too expensive to acquire, operate, and maintain. If a device with too little fidelity is specified, the training objectives may not be met which may leave aircrew ill-prepared to perform the real-world flying tasks, giving rise to the possibility of loss of hull and life. Furthermore, simply specifying a very high fidelity in a flight simulator does not guarantee that all training objectives can be met with such a device.

What is needed is a quantitative method to characterize and predict the effects of fidelity on pilot performance. Using this method, flight simulator designers can then perform cost-benefit trade-offs and flight training organizations can adjust the training tasks to achieve the selected training objectives with the least amount of expenditure.

Solution Approach

In this paper, we describe the use of the Cognitive Avionics Tool Set (CATS) to quantify the effects of simulator fidelity on neuro-cognitive and physiological patterns exhibited by pilots. CATS was developed by the Operator Performance Laboratory (OPL) under a NASA aviation safety project entitled "Operator State Sensor Investigations" with additional funding provided by the Office Of Naval Research (ONR) and industry [3-5]. Our hypothesis is that a simulator of the highest fidelity will generate a human neuro-cognitive and physiological response that is indistinguishable from the one observed in the real aircraft.

In addition to quantifying the effects of simulator fidelity itself, we hypothesize that CATS could be used to design flight simulator curricula that challenge pilots to such an extent that their neuro-cognitive and physiological responses (arousal levels) equal the intensity of the responses observed in the real airplane. We believe that training effectiveness in flight simulators depends on arousal levels that equal the ones observed in the real aircraft.

Apparatus

We developed a flight hardened human state sensor system for use on pilots flying real aircraft and flight simulators. We developed the necessary software to read the sensor state data, synchronize multiple channels into one stream of data, remove artifacts that arise at the sensor level, perform signal processing to characterize operator workload, and provide output to users in real-time and for after action review. The primary components of the overall software architecture is called the Cognitive Avionics Tool Set (CATS)[3, 4, 6].

In our experiment, the OPL L-29 research aircraft (Figure 1) and a matching flight simulator (Figure 2) provided the task stimulation at various levels of fidelity to the pilot who was fitted with a number of neuro-cognitive and physiological sensors including, electroencephalogram (EEG), electrocardiogram (ECG), respiration, and eye gaze tracking. As the pilot is performing a flight mission he/she responds to the cognitive demands of different mission task elements with characteristic neuro-cognitive and physiological patterns that are picked up by the sensors. The CATS processor continually reads the stream of data from the sensors, synchronizes those data into a unified system state vector, removes sensor artifacts, and performs signal processing such as fast Fourier transforms to provide the CATS operator state classifier with the data to calculate operator workload in real-time. This workload estimate is then transmitted to the plug-in of the instructor operator station which represents the primary user interface used by an instructor to monitor the training progress of a student. If desired, an instructor can open up CATS in a separate window to drill down into the data to investigate readings from individual sensors.

The experiment was performed on the OPL instrumented L-29 jet training aircraft (Figure 1) and a fixed base flight simulator (Figure 2). The content of the head-up and head-down displays in the flight simulator and the jet was identical. The aircraft was instrumented with an evaluation cockpit in the rear seat, integrated range instrumentation pods, a ground support infrastructure, and an operator monitoring and evaluation system. The aircraft was interconnected to a ground station using a range instrumentation datalink that can transmit in several formats, including the Advanced Range Data System (ARDS) protocol. This data link allowed for remote control of the experimental apparatus from our command and control trailer.

Figure 1. OPL's Instrumented L-29 Jet Trainer Aircraft

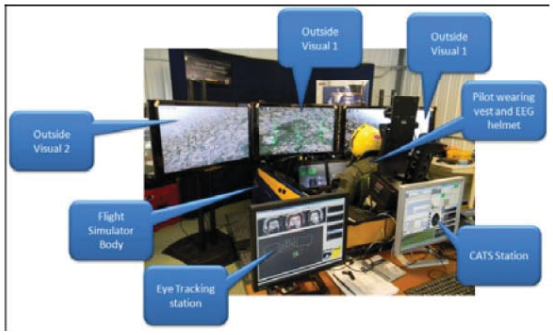

Figure 2. Fixed Base Flight Simulator

The flight simulator featured three channels of outside visuals, subtending a total of 120° lateral visual field of view (FOV) or around 40° per channel and a vertical field of view of 25 degrees. The outside visual (OSV) channels 2 and 3 were used to manipulate the fidelity of the flight simulator with low fidelity corresponding to the condition where OSV 2 and 3 were off and medium fidelity when OSV 2 and 3 were on. The high fidelity level corresponded to runs in the L-29 jet.

Both the HDD and the HUD in the jet subtend a lateral field of view of 22°. The symbology and imagery that was generated on the HUD was conformal to this field of view. This means that the HUD was a conformal window into the real world. From the crew station in the rear cockpit, the evaluation pilot had unrestricted visibility of the real world except for the HUD, which provided a conformal inset of OSV symbology.

Figure 3 (left) shows the front cockpit of the L-29 jet where the safety pilot (SP) operated. The SP performed all maneuvering on the ground, take-off, landing, and repositioning of the aircraft between runs. The SP used standard aircraft instruments to navigate in US airspace under FAR part 91 flight rules. Two VHF radios were available to allow the SP to simultaneously communicate with air traffic control (ATC) and the command and control ground station on separate frequencies. A side display touch screen called the Phase Tagger was available to the SP to start and stop the recorder, tag events to check the video data link integrity, and to check CATS and the integrity of the eye tracker.

The rear cockpit (Figure 3, right) was the crew station that the evaluation pilot (EP, experiment participant) occupied. A daylight readable 15 inch touch screen display was installed in the head-down position allowing presentation of any avionics symbology as per program requirements. The symbologies could be driven either with PC board dedicated avionics graphics processors. In this experiment, the symbologies were identical to the ones used in the simulator and represented an instrument panel. A daylight readable 15

inch touch screen in the head-up display (HUD) position provided the same outside visuals as the center display in the simulator. The lateral FOV of the HUD display was 22° which made the imagery displayed on it conformal with the real world. Therefore, a pilot in the rear crew station had an essentially unrestricted view of the surroundings, with the central 22° being a computer generated photorealistic inset and the remaining view being the real world.

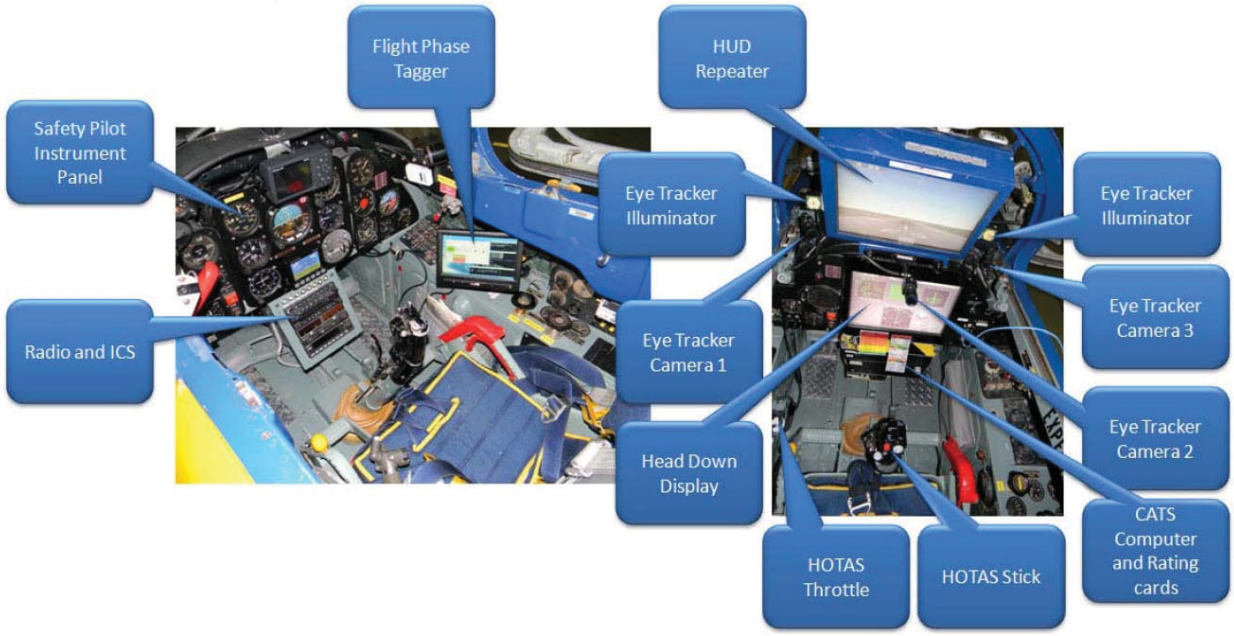

Figure 3. Front and Aft Cockpit of the L-29

To simplify the deployment of the neuro-cognitive and physiological sensors on the pilot we integrated the EEG electrodes in the liner of a flight helmet. The respiration belt and ECG electrodes were worn under the flight suit connecting to the peripheral electronics that are integrated in a pilot survival vest as shown in Figure 4. This level of integration provided for a ruggedized instrumentation package with a single point umbilical connection to the aircraft or flight simulator. The vest was designed from an ergonomics and flight safety point of view. The active electrode sensor cap was worn under the helmet with an additional soft helmet liner for wearer comfort. The EEG sensors were powered with batteries, which eliminated the need for an isolation transformer to ensure subject electrical safety.

Figure 4. Sensor Vest

One nice feature of the ActiCap electrode system is that each electrode has an LED, indicating the quality of the impedance of the sensor to skin interface. Before the experimenters put on the helmet over top of the sensor cap, a quick check of the LED status was performed to ensure acceptable impedance.

Figure 5 shows the overall data collection and analysis architecture that was used for this study. The figure illustrates the connections from the CATS sensor vest to the CART protocol processor. The CATS software can be run in real-time mode during data collection to provide the user with a detailed view of signal quality. However, running CATS during real-time is not necessary for experimental data collection, provided that the experimenters ensure that good quality data is being collected with CART. The CART GUI (sometimes referred to as the phase tagger) provides the experimenter with the ability to start and stop data collection for a particular run, or to advance the data collection indexed the next run. The recorded run index provides the user of CATS with the ability to query individual maneuvers during after action review. After the flight, the log files are extracted from the aircraft using either the datalink or a hardwired Ethernet hookup. The experimenter can then use the CATS output generator to create Google Earth files in the Keyhole Markup Language (KML) format of each run, with additional data overlays. This graphical depiction of the quality of the flight, including flight technical accuracy is an excellent way to perform after action review with students. For researchers, this tool is also an excellent way to determine root causes of strange performance effects. CATS generates detailed flight and mission performance plots and data sets that can be used for analysis of the accuracy of the flight. Batch mode processing in CATS generates summary data of the dependent variables for each run. This data can then be imported in additional packages such as Excel, Minitab, or Eureqa for analysis.

Figure 5 illustrates how we used the Eureqa data mining tool to generate workload equations for each of the 15 participants. These equations can be directly pasted into the expression parser of the workload gauges of CATS for subsequent real-time assessment of individualized workload.

EXPERIMENTAL DESIGN

We collected data in the OPL L 29 fighter jet trainer that served as the maximum fidelity upper baseline. Neuro-cognitive and physiological patterns observed under this maximum fidelity upper baseline were compared to the patterns observed in the flight simulator using a within subjects repeated measures experimental design.

We selected experimental tasks that included several flight maneuvers such as a simple climb, a holding pattern at a fix, a route with waypoint altitude clearance limits and speed assignments, and a wing-over maneuver that included several parameters such as pull-up point pulldown point, pitch angles, and bank angles, and an instrument approach (data not yet analyzed).

We used the number of variables that the pilot had to control for each maneuver as an indicator of the difficulty level of that maneuver as shown in Table 1.

Table 1. Assignment of Maneuver Difficulty to Task

Maneuver	Assumed Difficulty Level
Climb	1
Hold	2
Route	4
Wing Over	6

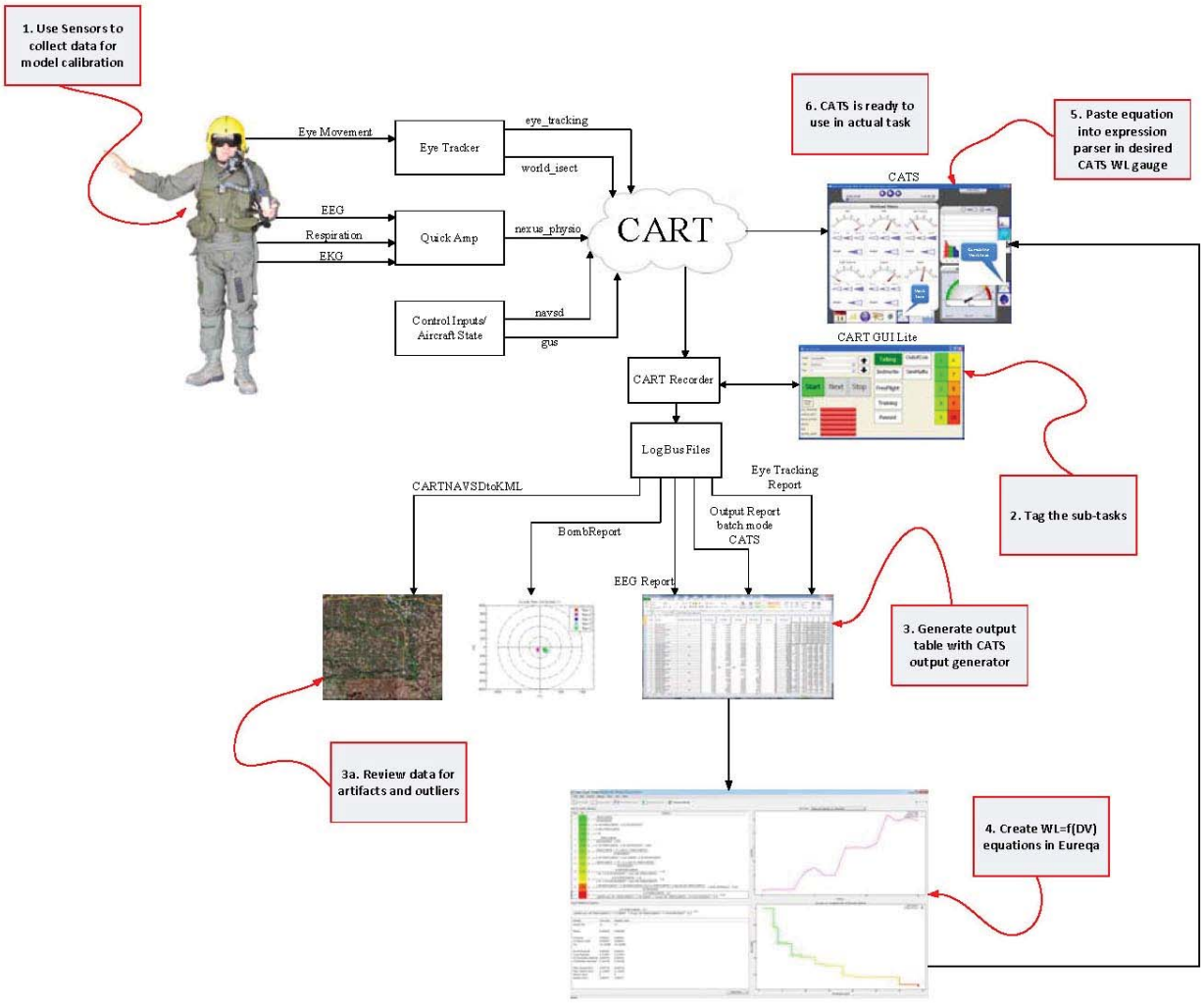

Figure 5. CART and CATS Data Collection and Analysis System

The dependent measures in CATS comprised in excess of 380 variables derived from EEG, ECG, eye movement, and flight technical performance. The EEG metrics consisted of power values in different clinical bands (delta, theta, alpha, beta, and gamma) for different scalp topographical regions (EOG, midline, sensorimotor, occipital), and different summary statistics (average, minimum, maximum, RMS, standard deviation). The ECG metrics consisted of straight heart rate, the percentage of heartbeats outside of a 20 ms or 50 ms window, and short-term heart rate trend. Eye fixation metrics included the number of fixations in areas of interest, fixation duration, and distance between subsequent fixations. There are many task specific flight technical measures that were used including cross track error, vertical track error, speed error, climb angle and descent angle.

A total of 15 subjects were used in this study. This pool of subjects was divided into three groups of five each. Group 1 consisted of those pilots who flew the simulator using only one channel of outside visuals, Group 2 flew the simulator with three outside visual channels, and Group 3 flew their mission in the real aircraft. Each pilot participant performed five replications of each run.

RESULTS

Effect of Fidelity on Selected Variables

In this paper we will focus on the individualized operator state models. Only a small selection of physiological data is discussed herein. Additional results can be found in [2]. Figure 6 shows the effect of simulator fidelity on heart rate using a cumulative histogram. The leftmost trace indicates a heart rate distribution for those pilots who flew their mission in the simulator using three channels of outside visuals with no motion. The three outside visual channels provided the pilot with sufficient lateral visual information to allow performance of the maneuvering tasks with relative ease. This is reflected in a lower heart rate. With no change other than turning off the two peripheral outside visual displays and flying the mission with only one channel of outside visuals, the heart rate increased statistically significantly. This is a clear indication that the pilots had to compensate for the lack of field of view during the maneuvering tasks using additional cognitive resources in the process. The increase in simulator fidelity reduced the level of cognitive loading because more of the necessary information is available in the three channel simulator condition.

One could argue that the flights performed in the real aircraft should result in even less cognitive workload and arousal as the visual display is volumetric and 360° at real-world resolution. However, this is not what we found. Instead, we found that the heart rate was significantly higher in the real aircraft when compared to both simulator conditions. This, of course, makes complete sense as not only the visuals change, but also the motion dynamics, acoustics, and the knowledge that one is in fact in a real airplane flying at high speeds and high altitudes. Pilots flying in the fixed base simulator did not feel the effects of acceleration, whereas pilots in the aircraft did. We saw many more turn overshoots in the aircraft when compared to the simulator. The pilots who were participated in this study had not flown nimble acrobatic jet aircraft before. These participants were therefore highly aroused in anticipation of the mission on hand. Flying the aircraft also provided additional stimulation in the olfactory, auditory, and proprioceptive stimulus dimensions. Therefore, we feel that the heart rate increase observed for the aircraft sorties in Figure 6 are consistent with our expectations. A similar effect was found in EEG (Figure 7).

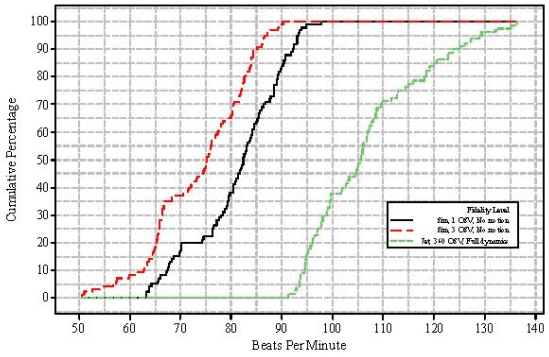

N=15 participants at 5 replications. ANOVA: $F_{3,42}$=269.06, p<0.001. Pairwise T: Level 1 vs. Level 2 T=-5.395, p=0.00001, Level 1 vs. Level 3 T=17.354, p=0.00001, Level 2 vs. Level 3 T=22.44, p<0.00001

Figure 6. Beats per Minute Effect for Simulator Fidelity Levels

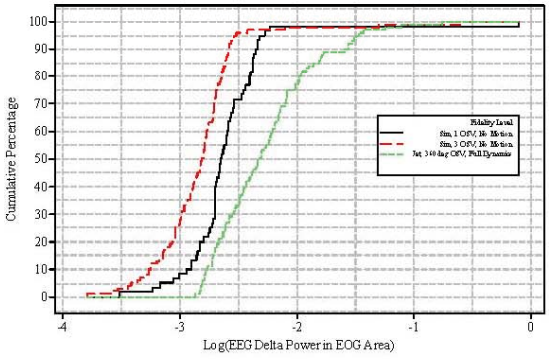

N=15 participants at 5 replications. ANOVA: $F_{3,42}$=49.35, p<0.0001. Pairwise T: Level 1 vs. Level 2 T=-3.442, p=0.0017, Level 1 vs. Level 3 T=5.123, p=0.00001, Level 2 vs. Level 3 T=9.891, p<0.00001

Figure 7. Log of EEG Power in EOG Area for Fidelity

Personalized Workload Models

We used the study data to build individualized workload equations, separately for each participant. We used replications 1,2,4, and 5 to build the workload model and we validated the resulting equations against data from replication 3. This sequence was chosen because we believe that replications 1 and 2 were in the steep part of the learning curve and replications 4 and 5 were in the flat part of the learning curve. Combined, this training data set represented a fairly neutral learning condition. The Replication 3 validation data point was thought to be in the neutral region between the steep and flat part of the learning curve. A total of 15 equations (Table 3) were generated using Eureqa and entered into Excel for validation against the third application data set. The resulting predicted task difficulty level was then plotted against the actual task difficulty level as shown in Figure 8. The correlation between the actual and predicted data set was 0.888. We feel this is a fairly respectable result in terms of accuracy of prediction.

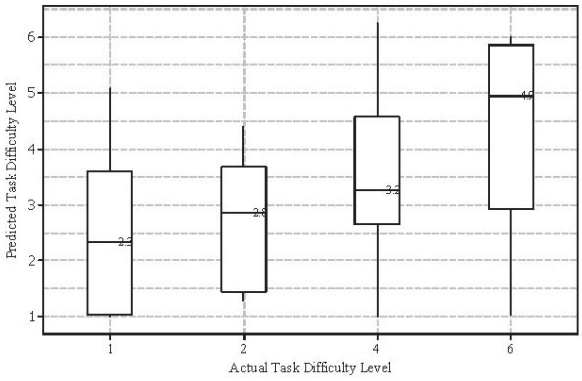

Correlation between actual and predicted data is 0.888

Figure 8. Predicted vs. Actual Task Difficulty Level using Neurocognitive and Physiological Measures

The workload models shown in Table 3 were developed by using Eureqa to determine the significant variables to construct a nonlinear regression model for each participant. An explanation of the variable names is given in Table 2

Table 2. Main Variables used in Workload Prediction Models

Variable	Meaning
PERCLOBPM	Percent difference of task heartbeat compared to rest
LPNN20	Log percentage of heartbeats falling outside of a 20 ms inter-beat interval
LBLM	Log beta low midline EEG power
LBO	Log beta occipital EEG power
LDS	Log delta sensory motor EEG power
LDM	Log delta midline EEG power
HUDFIXDIST	Distance between subsequent eye fixations to the HUD
HUDFDMEAN	Mean duration of eye fixations made to the HUD

DISCUSSION

Four flight tasks of increasing levels of difficulty were used in 15 pilots to elicit a range of workload responses. Neuro-cognitive and physiological measures were collected for three levels of simulator fidelity (low, medium, high) using the Cognitive Avionics Tool Set (CATS). Nonlinear closed form models for workload prediction were generated based on these data for the various mission task elements

Our data indicate that there is a significant difference in the neuro-cognitive and physiological patterns obtained from pilots flying a fixed base flight simulator when compared to flying the real aircraft. We also found that the real aircraft provided considerably more cognitive arousal to the pilots used in our experiment when

compared to the level of arousal that was provided by the flight simulator. We discovered that factors such as the extent of the field of view of the outside visuals in a flight simulator can considerably affect neuro-cognitive and physiological patterns which can be discriminated with the algorithms integrated in CATS.

Based on our results, it seems that simple heart rate is a relatively good predictor of cognitive workload, even for short tasks with dynamic changes in cognitive loading. Additionally, we found that models which use a wide range of physiological and neuro-cognitive measures can further boost the accuracy of the workload prediction. By comparing the physiological and neuro-cognitive response of pilots in a simulated environment with the corresponding response in real aircraft, it was possible to generate measures of performance that track with the fidelity of a virtual environment.

Based on our data, we can conclude with confidence that pilots flying the aircraft struggled more and generated larger flight technical errors when compared to pilots flying the simulator. However, the percentage of improvement from the first to the fifth replication was much larger in the aircraft than it was in the flight simulator. We believe that the multisensory stimulation in the aircraft aids pilots in improving flight control inputs from one replication to the next. Operators of fixed base training flight simulators should consider increasing task difficulty beyond what is expected in the real aircraft. This increase in task difficulty will increase the trainee's arousal level thereby generating neuro-cognitive and physiological engagement levels approaching those observed in the real aircraft.

This study is limited to one incarnation of a fixed base flight simulator and a study with a relatively small sample size. Without performing a study in a high-end motion base simulator, we simply cannot hypothesize on the performance that one would observe in a high-end simulation device. However, it appears that the multisensory stimulation experienced in the real aircraft aids the pilot in refining their sensorimotor skills throughout about five replications.

REFERENCES

1. Alexander, A., L. Brunye, and T. Weil. *From Gaming to Training: A Review of Studies on Fidelity, Immersion, Presence, and Buy-in and Their Effects on Transfer in PC-Based Simulations and Games*. 2005; Available from: http://www.darwars.org/downloads/DARWARS%20Paper%2012205.pdf.
2. Schnell, T., A. Postnikov, and N. Hamel, *Neuroergonomic Assessment of Simulator Fidelity in an Aviation Centric Live Virtual Constructive (LVC) Application*, in *HCI International 2011*. 2011, Springer: Hilton Orlando Bonnet Creek, Orlando, Florida, USA.
3. Schnell, T., M. Keller, and T. Macuda, *Application of the Cognitive Avionics Tool Set (CATS) in Airborne Operator State Classification.* Augmented Cognition International Conference, 2007.
4. Schnell, T., M. Keller, and P. Poolman. *Neurophysiological workload assessment in flight*. in *Digital Avionics Systems Conference, 2008. DASC 2008. IEEE/AIAA 27th*. 2008.
5. Schnell, T., T. Macuda, and M. Keller, *Sensor Integration to Characterize Operator State*, in *Augmented Cognition; A Practitioner's Guide*, D.D.S.K.M. Stanney, Editor. 2008, Human Factors and Ergonomics Society. p. 33.
6. Schnell, T., J.E. Melzer, and S.J. Robbins. *The cognitive pilot helmet: enabling pilot-aware smart avionics*. in *Head- and Helmet-Mounted Displays XIV: Design and Applications, April 16, 2009 - April 16, 2009*. 2009. Orlando, FL, United states: SPIE.

Table 3. Task Difficulty Prediction Models for CAS Task

Subject	Task Difficulty=f(Dependent Variables)	R^2	Fitness	
1	1.3184637*cos(PERCLOBPM + 1.3555878*LBLM) + 0.12370914*PERCLOBPM + 0.51329815*LBLM + 1.6968185*sin(221.40964*LBLM) - 1.1071174*sin(2.0060091*PERCLOBPM) - 0.059559464	0.991	0.059	Simulator, 1 C hannel of OSV
2	1.0827115 + (3.3491788*LPNN20 + 0.28201574*PERCLOBPM + sin(69.19706*LBO) + 2.353423	0.96	0.149	
3	0.84847742 + (0.16712549*PERCLOBPM*PERCLOBPM + -0.91743886*HUDFIXDIST*cos(-9.3917542*PERCLOBPM)*cos(-9.3917542*PERCLOBPM)/HUDFDMEAN - 25.426651*cos(-9.3917542*PERCLOBPM)*cos(-9.3917542*PERCLOBPM)*cos(PERCLOBPM - 1.4302194*HUDFDMEAN))/HUDFIXDIST	0.99	0.061	
4	1.564743 + HUDFDMEAN + 0.34546053*PERCLOBPM + 1.2832386*cos(LDM*LBLM) + 0.37645277*cos(1.1469964*PERCLOBPM)*cos(1.4169006*PERCLOBPM*PERCLOBPM) + 2.9303737*HUDFDMEAN*cos(1.1469964*PERCLOBPM) - 0.46708772*cos(1.4169006*PERCLOBPM*PERCLOBPM)	0.996	0.045	
5	2.7095852 + cos(PERCLOBPM)*cos(PERCLOBPM - 4.4980625e-5)/(0.11290019 + 1.5396878/(PERCLOBPM - 4.4980625e-5)) + 0.91720986*cos(PERCLOBPM) - 0.75311863*cos(PERCLOBPM - 4.4980625e-5)*cos(2.763207*PERCLOBPM*PERCLOBPM) - 0.045648079/sin(PERCLOBPM) - 3.929251*HUDFDMEAN	0.991	0.049	
6	5.8512836 + 2.6331587*cos(10.289939*PERCLOBPM)/(PERCLOBPM - 3.6436858) + (2.5140517*HUDFIXDIST*sin(sin(14.251148*LBO)) - 22.866884*sin(sin(14.251148*LBO)))/(cos(PERCLOBPM - 3.6436858/PERCLOBPM) + PERCLOBPM - 4.1335578)	0.995	0.041	Simulator, 3 C hannels of OSV
7	2.609494 + sin(0.20168348*PERCLOBPM) + 0.20168348*PERCLOBPM*HUDFDMEAN*sin(0.20168348*PERCLOBPM)*sin(-3.2543337*LBLM/LPNN20)*sin(-3.2543337*LBLM/LPNN20) + 11.91309*HUDFDMEAN*HUDFDMEAN*HUDFDMEAN*sin(-3.2543337*LBLM/LPNN20) +	0.975	0.081	
8	0.27726284 + 5.3854728*cos(LTS) + 5.3854728*HUDFDMEAN*cos(HUDFDMEAN) + 0.64272124*sin(-2959.6062*LBO) + 1.5181508*sin(-0.17662553*HUDFIXDIST)/(sin(-626.79443*LBO) - 0.965011)	0.997	0.036	
9	2.8691647 + sin(4.32651*LDS + 2.6206877*PERCLOBPM*LDS) + 2.6206877*LDS*cos(LDS*LDM) + 9.831584*cos(LDS*LDM) - 3.0779896*log(PERCLOBPM)*cos(LDS*LDM) - 0.58662623/LDS - 0.14015104*PERCLOBPM	0.97	0.104	
10	3.2809136 + 1578.9419/(-1252.537*LDM) + 2.6978884*cos(106.14892*LDM) + 0.68518925*cos(-1252.537*LDM) + 3.3517282*sin(108.99526*LDM) - 1.4094001*cos(196.23761*LDM)*cos(106.14892*LDM)	0.993	0.044	
11	3.2083549 + 0.31052729*cos(231.55759*HUDFIXDIST) + 2.2928617*cos(-10.254387*HUDFIXDIST) + 0.22617097*HUDFIXDIST*cos(-18.568399*LDM)*cos(-10.222954*HUDFIXDIST*HUDFIXDIST) + (3.2083549 + 0.31052729*cos(231.55759*HUDFIXDIST) + 2.2928617*cos(-10.254387*HUDFIXDIST) +	0.998	0.024	Aircraft
12	4.3274031 + 2.0209646*sin(0.13923776*PERCLOBPM) + 2.3252544*sin(0.12731959*PERCLOBPM)*sin(2.7443035*PERCLOBPM) - 1.5827621*sin(0.12731959*PERCLOBPM)*sin(2.2408776*PERCLOBPM)*sin(2.7443035*PERCLOBPM) - sin(2.2408776*PERCLOBPM)*cos(sin(0.13923776*PERCLOBPM))	0.98	0.058	
13	1.2922051*sin(103.67542/LPNN20) + 0.13030657*PERCLOBPM + 0.026240172*PERCLOBPM/LPNN20 + cos(sin(103.67542/LPNN20)) - 1.7087533*sin(56.959488/LPNN20)*cos(0.13030657*PERCLOBPM + 1.2922051/(0.13030657*PERCLOBPM + 0.026240172*PERCLOBPM/LPNN20)) - 0.72068655	0.994	0.058	
14	(-2.6239846*PERCLOBPM - 217.39574)/(LDEOG*cos(-386.85562*PERCLOBPM) + 3.2971733*LDEOG - 1.7448196*cos(-587.14429*PERCLOBPM) - 0.57358128*HUDFIXDIST - 11.827497) - 8.500103	0.99	0.068	
15	0.0022779282*PERCLOBPM*PERCLOBPM + 3.7092943*LDS + 2.5593133*HUDFDMEAN - 7.2671909*LTS - 1.4026718*log(0.0019029471*PERCLOBPM*PERCLOBPM)*sin(4.7368174*PERCLOBPM*PERCLOBPM) - 23.494602	0.988	0.072	